Proceedings of the 10th World Congress on Momentum, Heat and Mass Transfer (MHMT 2025)
Barcelona, Spain - April, 2025
Paper No. ICMFHT 140
DOI: 10.11159/icmfht25.140

Twin-Fluid Nozzle for FCC Riser: Atomization and Spray Dynamics

Deepak Kumar[1], Abhishek Verma[1], Abhijit Kushari[1], Pramod Kumar[2], Hemant Mishra[2]
[1]Indian Institute of Technology Kanpur
Department of Aerospace Engineering, Kanpur, India
deepakkr@iitk.ac.in; abhishv@iitk.ac.in; akushari@iitk.ac.in
[2]Hindustan Petroleum Corporation Limited
Bangalore, India

Abstract - Fluidized Bed Catalytic Cracking is a key conversion process in most refineries, transforming low-value heavy components of crude oil into high-value light products. The FCC unit consists of two main reactors—a riser and a regenerator. Typically, vacuum gas oil (VGO) serves as the feedstock, which is converted into valuable products such as LPG, gasoline, and diesel. The feed nozzle system, located at the base of the riser, injects VGO as liquid droplets. These droplets come into contact with a hot regenerated catalyst drawn from the regenerator, ensuring efficient mixing. Effective atomization from the feed nozzles is crucial for maximizing contact between the hydrocarbon feed and the catalyst. Most modern FCC nozzles are twin-fluid atomizers, which utilize pressurized gas to enhance fuel atomization. This study focuses on the spray characteristics of a specially designed nozzle for riser applications. A detailed experimental analysis is conducted to determine the optimal operating parameters for the nozzles. The section-wise averaged Sauter Mean Diameter decreases with increasing Air-to-Liquid Ratio (ALR) and closely follows a log-normal distribution. However, the overall section-wise average droplet velocity does not appear to follow a normal distribution.

***Keywords*:** FCC riser, Twin fluid injector, SMD, PDPA.

1. Introduction

Fluid Catalytic Cracking is the primary conversion of the feed (low-grade oil) into a variety of high-value products [2]. It is composed of a riser and a regenerator unit. The feed atomize system is based on the bottom of the riser. The feed (vacuum gas oil) is supplied into the riser with the help of an atomizer in the form of fine droplets. The feed atomized system plays a major role in the modern FCC riser design and fine atomization from the feed atomized system ensures mixing thoroughly with the hot catalyst [3]. In modern FCC, a highly active zeolite catalyst is used. Due to this, the reaction time has been reduced to very few seconds. As soon as liquid hydrocarbon feedstock is vaporized, and mixed, the feed vaporization must take place so quickly for catalytic cracking reaction to complete in a few seconds [4,5]. On the other hand, the feedstock is heavy oil having higher viscosity and boiling points. Hereof, better atomization of heavy feed is desired to convert into very tiny droplets. So that the vaporization of the heavy and viscous feed must take place within a few seconds. Different types of arrangements are used to improve the quality of atomization or to improve the performance of atomization units. These atomizers are widely used in many spraying systems for domestic and industrial applications. These injectors are categorized as Air-blast and Air-assist atomizers based on the quantity and relative velocity of the gas phase. Depending on configurations, these injectors are further divided into external and internal mixing type injectors. Most of the FCC nozzle systems used in the modern FCC units Twin-fluid atomizers are widely used to atomize the liquid.

In the Fluidized Bed Catalytic Cracking (FCC) process, twin fluid injectors are successfully used for the last fifty years without any hindrance. Guo et al. [6] found that, at the given gas pressure, the spray angle gradually increases with an increase of the liquid phase velocity, whereas, at the given liquid pressure, the spray angle decreases with an increase of the gas pressure. Chen and Lefebvre [7] observed that for low ambient pressures, the value of the spray cone angle increases continuously with the increase of the gas to the liquid mass ratio (GLR), whereas at higher pressures, it has a maximum value at an intermediate GLR. They explained that the decrease in cone angle at high GLRs is caused by the transition of the two-phase flow inside the atomizer exit orifice. Kushari et al. [8, 9] investigated that the small amount of airflow rate into the liquid stream is sufficient to attain the atomization and suggested that the investigated injector could be used to control flow rate and spray characteristics independently. Also, concluded that the size of the droplets decreases with a decrease in the injection area of air as well as an increase in the injector's length. Ju et al. [10] investigated air-assisted atomizer for heavy oils using sonic compressed air at 0.4 MPa to control fuel flow rate and to have separate control of fuel flow rate with a fine spray and desirable flame length. Kin et al. [11] Investigated the effect of mixing chamber geometry by visualization the flow pattern and presented that atomization mainly occurred due to the breakup of liquid film on the top and side surface of the mixing chamber. Nguyen et al. [12] studied two types of atomizers. They observed that volume median drop diameters as low as 10 µm at ALR less than unity and proposed a relation for volume drop diameter with atomizer geometry and operating conditions. Kufferath et al. [13] showed that the flow characteristics have a strong influence on the radial distribution of the Sauter mean diameter and mass density. They also showed that maximum D_{32} for laminar velocity is found on the spray axes whereas, in turbulent flow, it was nearly radial profiles. Karnawat et al. [14, 15] evaluated the performance of twin fluid atomizers in a controlled fashion. Ferreira et al. [16, 17] found that SMD decreases upon increasing airflow rate and, the smallest SMD is produced by the channel diameter under choked conditions and, presented design optimization for twin fluid injector for heavy oils. Lal et al. [18] reported controlled atomization for twin fluid atomizers especially for the use of fire suppression applications. Zheu et al. [19] focused on a single-hole Y-jet nozzle with a high mass flow rate. They showed that the mean diameter of the Y Y-type injector is a non-linear function of ALR and decreases with increasing ALR.

the current study, a further extension of our previous work Kumar et al. [20]. The performance of the injectors was studied experimentally in detail with a wide range of operating conditions. The objective of this study is to evaluate the atomization spray of the 3-hole and 4-hole injectors and their comparative atomization properties were also studied. The detailed measurements were performed in the present study by the PDPA technique at various downstream positions for both the injectors.

2. Experimental setup and measurements methodology

The experimental setup, injector design for FCC riser, and measurement methodology are described in the following subsections.

2.1. Twin Fluid injector for FCC riser

The twin-fluid atomizer used in the present study is illustrated in Fig. 1. Two different nozzle configurations, one with three orifices and another with four orifices, are investigated. Water and air serve as the working fluids in this study.
A central tube with a 6 mm diameter is used to supply water into the atomizer. At the end of this tube, two 2 mm diameter holes allow water to enter the atomizer assembly. This central tube is enclosed within a 12 mm diameter hollow tube, through which air is supplied. To accelerate the airflow inside the hollow tube, a jet plate with four 1.5 mm diameter holes is incorporated. Additionally, two 2 mm diameter holes are positioned 18 mm above the central tube's exit to introduce a small amount of air into the central tube, thereby enhancing water flow acceleration. An impactor plate is placed downstream of the central tube exit. The accelerated liquid jet impinges on this plate, leading to droplet breakup. The generated droplets are then carried downstream by the airflow, passing through six rectangular slits, each measuring 4.5 mm × 2 mm, positioned around the impactor plate.

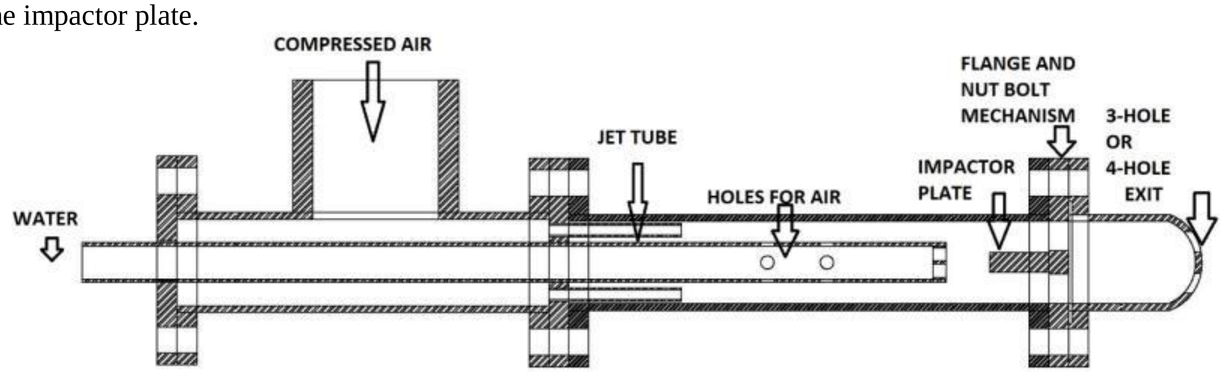

Fig. 1. Schematic of Injector.

2.2. Measurement's methodology

The overall assembled injector was mounted on the top of the spray chamber (of 0.75 m X 0.75 m X 1.25 m in size) provided with optical access for the PDPA measurements. The schematic of the experimental rig is shown in Fig. 2. Honeycomb structure was placed at the bottom surface of the spray chamber to avoid mist formation in the test section and to stop the interference of this mist with the main formed spray and the optical measurements. Water is supplied with the help of compressed air from the water storage tank. It is controlled by a pressure regulating valve and monitored by the rotameter. The air is supplied by a laboratory high-pressure line and is monitored by a rotameter, and a needle valve, and controlled by a pressure regulating valve. Density corrections were made by closely monitoring the pressure by using a pressure gauge of the accuracy of ±1 % of full scale.10-point font size.

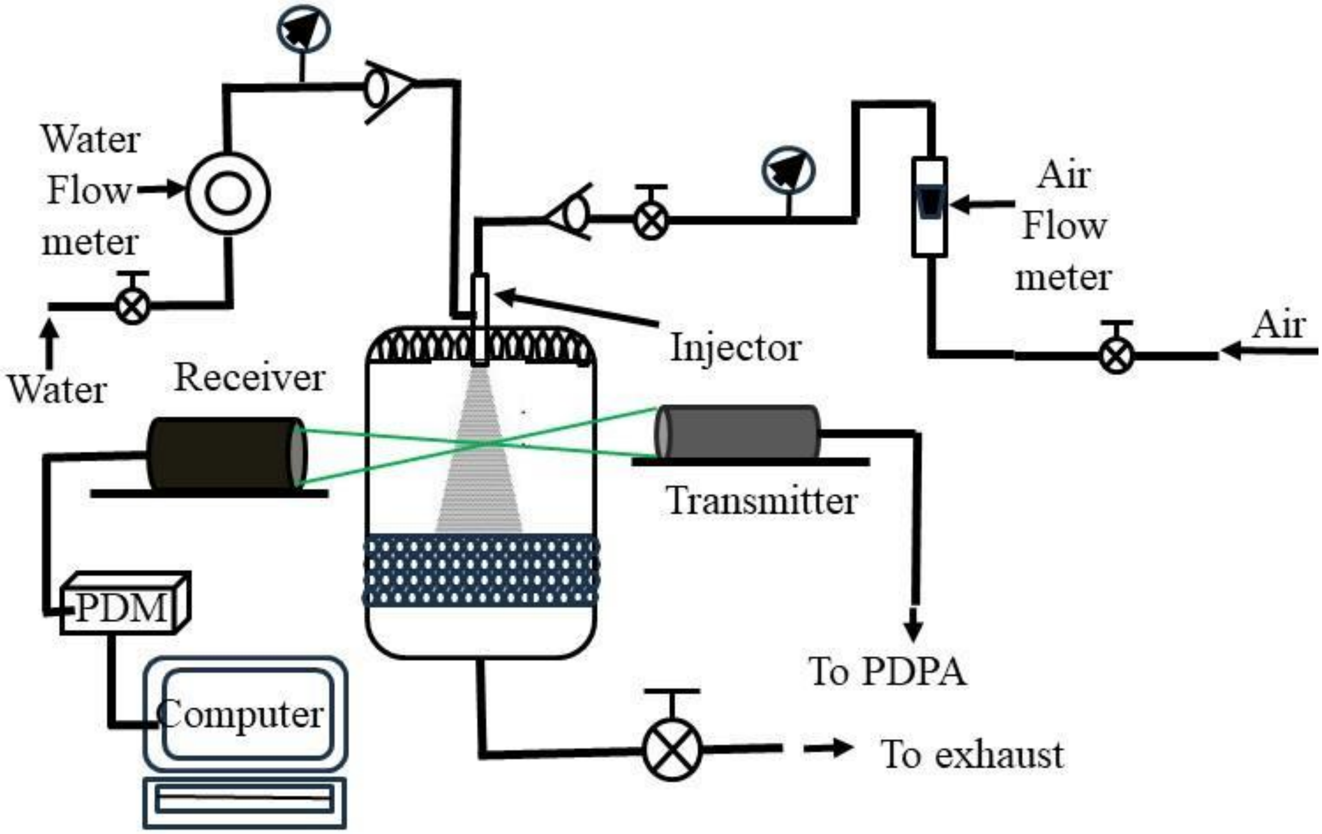

Fig. 2.Experimental setup.

2.3. Operating conditions

The operating conditions for evaluating spray characteristics were selected independently for air and water flow rates. Droplet size and velocity were analyzed using PDPA measurements at two water flow rates and three airflow rates. The operating conditions for the 4-hole and 3-hole injectors are detailed in Table 1 and Table 2, respectively. Given the differences in exit areas between the two injectors, only minor variations were observed.

Table 1. Operating conditions for the 4-hole injector.

S. No.	Q (lpm)	$\dot{P}_l$ (bar)	P_a (bar)	$\dot{m}_a$ (kg/s)	$\dot{m}_l$ (kg/s)	ALR
1.	1	0.05	1.1	0.0015	0.017	0.085
2.	1.5	0.1	1.2	0.0015	0.026	0.058
3.	1	0.1	2.1	0.0029	0.017	0.165
4.	1.5	0.45	2.3	0.0029	0.026	0.111
5.	1	0.5	3.7	0.0048	0.017	0.28
6.	1.5	0.8	3.8	0.0048	0.026	0.19

Table 2. Operating conditions for the 3-hole injector.

S. No.	Q (lpm)	P_l (bar)	P_a (bar)	$\dot{m}_a$ (kg/s)	$\dot{m}_l$ (kg/s)	ALR
1.	1	0.2	1	0.0014	0.017	0.083
2.	1.5	0.3	1.1	0.0015	0.026	0.057
3.	1	0.2	2	0.0028	0.017	0.163
4.	1.5	0.5	2.2	0.0029	0.026	0.112
5.	1	1	3.7	0.0048	0.017	0.28
6.	1.5	1.2	3.9	0.0049	0.026	0.19

2.4. Measurements points and grids

The size and velocity measurements were performed along with spray centerline as well as across the section for both the injectors. Along the centerline, the measurement was performed after a 10 mm interval start at a position 10 mm downstream of the nozzle tip to 180 mm. Across the cross-section at 110 mm downstream, the grids x=-24:4:24 and y=-20:4:20 measurements were performed for both the injectors. These locations are shown in Fig. 3. The SMD and velocity measurements for both 3-hole and 4-hole injectors along the centerline as well as section-wise are discussed below.

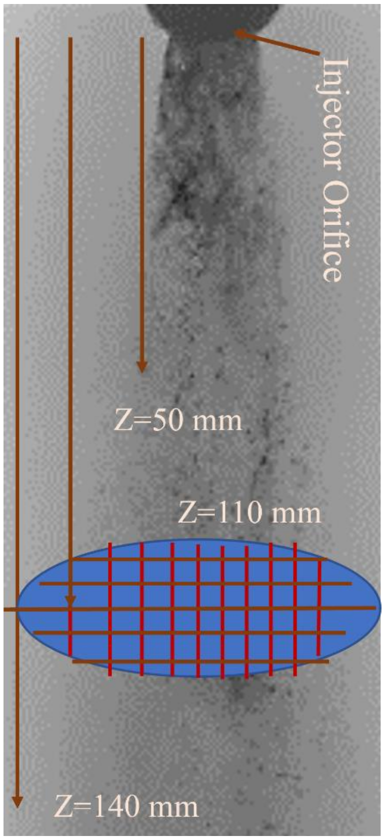

Fig. 3. PDPA measurement's location points.

3. Results

This section presents the results obtained from two types of injectors used in fluidized bed catalytic cracking. The spray characteristics of the injectors are analyzed based on the Sauter Mean Diameter (SMD) distribution. To provide a comprehensive representation of SMD and droplet velocity, measurements were conducted along the spray centreline and across a section. The findings offer a clear insight into the distribution of spray droplets.

Centerline distribution

Figure 4 illustrates the correlation between droplet size and velocity at mw = 0.017 kg/s and ma = 0.0048 kg/s for both for both 3-hole and 4-hole injectors across different downstream locations. A consistent trend is observed across all locations, locations, where smaller droplets exhibit higher velocities, while larger droplets move more slowly. This behavior results results from momentum transfer and aerodynamic drag, as smaller droplets decelerate more rapidly due to their higher surface-area-to-mass ratio. For the 4-hole injector, the droplet size distribution is more uniform, with a higher concentration of fine droplets (<60 µm). The velocity remains relatively consistent between 30–70 m/s, and the presence of fewer large droplets indicates better atomization efficiency, contributing to a more homogeneous spray. As the spray evolves downstream (50 mm to 140 mm), droplet velocity decreases due to momentum loss from drag and dispersion. In contrast, the 3-hole injector exhibits a broader velocity spread for larger droplets, indicating a more heterogeneous spray pattern. A higher number of large droplets (>80 µm) is observed at greater distances (110 mm, 140 mm), suggesting slower breakup and reduced energy dissipation. At 50 mm, both injectors display a dense cloud of fine droplets with higher initial velocities. However, by 110 mm, the 4-hole injector maintains a more uniform distribution of larger droplets, whereas the 3-hole injector shows an increasing dominance of larger droplets. At 140 mm, the velocity of large droplets (>100 µm) remains high in the 3-hole injector, whereas in the 4-hole injector, velocity decreases more smoothly, indicating better atomization and mixing. The 4-hole injector enhances atomization efficiency through higher turbulence and shear forces, resulting in smaller, more uniform droplets. In contrast, the 3-hole injector, with fewer outlets, generates larger primary droplets that take longer to break up. Smaller droplets lose velocity more rapidly due to higher aerodynamic drag, while larger droplets retain momentum, particularly in the 3-hole injector, where interaction with the airflow is less effective. Overall, the 4-hole injector produces a more dispersed spray with a wider velocity range, whereas the 3-hole injector forms a more clustered spray of larger droplets, leading to non-uniform mixing.

Section-wise distribution

The size and velocity contours are evaluated at a cross-section located at 110 mm downstream of the atomizer exit. In the Fig. 5, the spray center is located at X= 28 and Y = 30 for (a) and X= 27 and Y= 20 (b). Fig. 5 a) represent the contour of SMD for 4-hole at $m_{w=}$ 0.017 kg/s, m_a = 0.0015 kg/s. While 5 b) represent the contour of SMD for 3-hole at $m_{w=}$ 0.017 kg/s, m_a = 0.0015 kg/s. From the figures, it can be observed that the droplet SMD increases as one moves away from the spray centerline. At the spray centerline, the SMD is in the range of 84 µm to 88µm. On moving further away from the spray centerline axis, the SMD is found to be increasing reaching up to 115µm at the spray edges. But in, as the water flow rate is increased for the same air mass flow rate, the same trend is observed. As expected, the droplet diameter is larger in (b) compared to (a). From the velocity plots in Fig.6 and, it is seen that the axial velocity corresponding to the larger they have higher radial velocities than the smaller droplets. Also, at the spray boundaries, the SMD appears to decrease by a small value. This may be due to the shear effect of the spray boundaries and the quiescent air. At the spray edges, SMD is decreasing slightly, possibly due to the shear action between the quiescent air and the droplets at the spray boundaries. in this case, also the SMD is found to be increasing across the spray diameter. Although an eccentric pattern is observed in this case whereas the region with lower SMD is slightly moved in the Y direction. Also, it is observed that the SMD is also lower than that for a four holes injector nozzle. This can be expected as it is seen from the velocity plots Fig. 6 that the velocity of the droplets is increasing for three holes injector for the same operating conditions. This increase in the droplet velocity can enhance the secondary atomization. 6 a), represent the contour of axial mean velocity for 4-hole at $m_{w=}$ 0.017 kg/s, m_a = 0.0015 kg/s. While 6 b) represent the contour of axial mean velocity for 3-hole at $m_{w=}$ 0.017 kg/s, m_a = 0.0015 kg/s. The axial velocity is high at the center of the spray and is decreasing as the spray diameter is increasing. But the radial velocity is negligible compared to the axial velocities of the droplets. The figure shows that as the water flow rate is increased for the same airflow rates, there is an increase in the droplet velocities also, although the maximum velocity in the case is 11 m/s which is very close to the maximum velocity for the previous case a), which is around 9m/s. The behavior of averaged section droplet size and averaged section mean velocity at a particular section (110 downstream) yet to study. This can be seen in Fig. 7 and Fig. 8. Fig. 7 shows a comparison of section Sauter mean diameter with different ALR's for both the type injectors. Section SMD decreases with an increase in ALR. Both types of injectors show a decreasing trend. Here, it can also be seen that section SMD for the 3-hole injector is lower than the 4-hole injector.

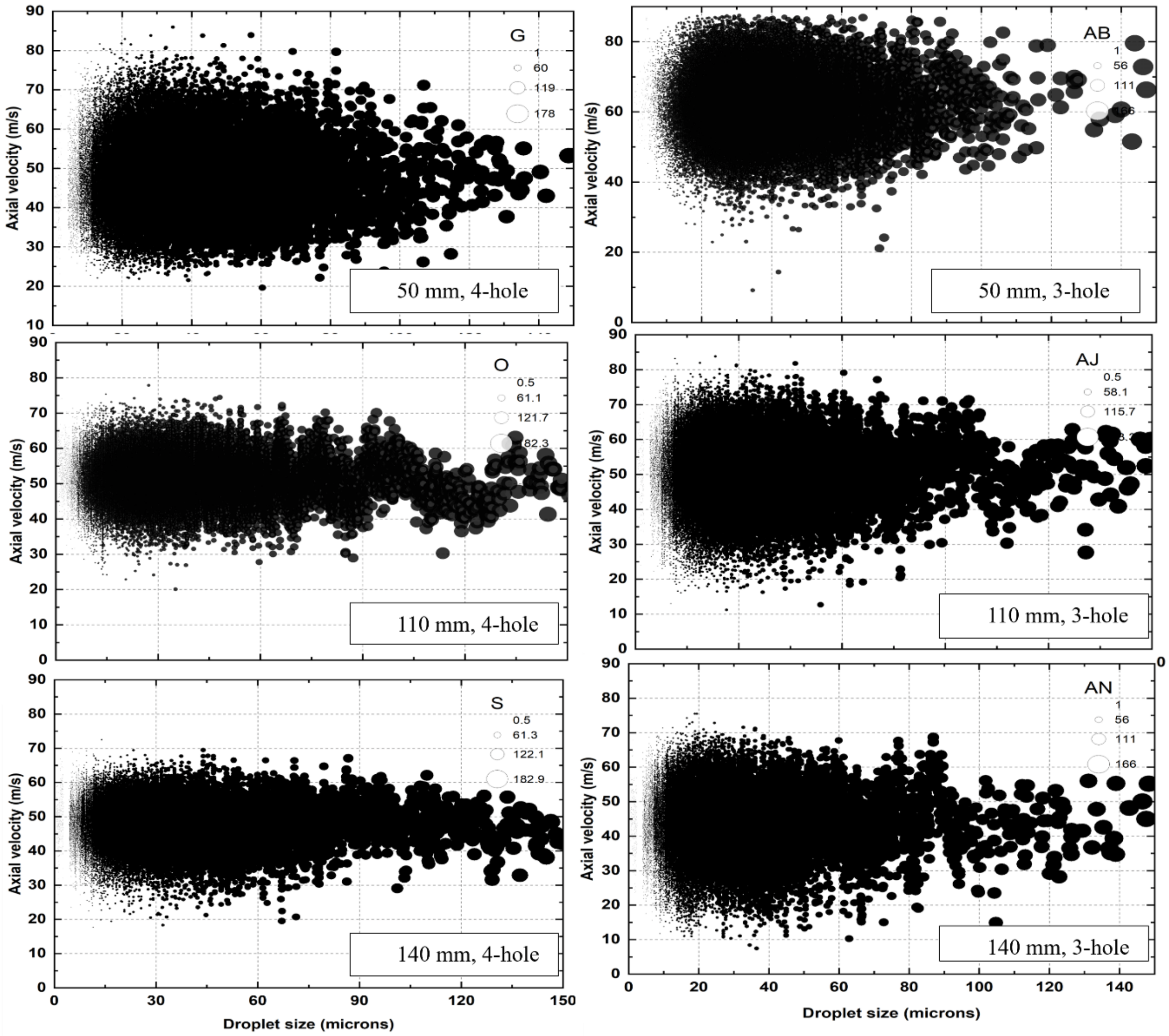

Fig. 4. Droplet size and velocity distribution at mw=0.017 kg/s and ma=0.0048 kg/s.

Fig. 8 shows the comparison between the section mean velocity for both the injectors at the various value of ALR at 110mm downstream position from the injection tip. The section mean velocity increases with increased ALR for a 3-hole injector while the variation for 4-hole shows some randomness. Section mean velocity attained from the 3-hole injector is higher than that of attain from the 4-hole injector. Fig. 7 shows a section-wise averaged droplet size distribution at various ALR values. The first two rows represent the overall size distribution at a section 110 mm downstream position from the injection tip for the 3- hole type injector and the other two represent the same for the 4-hole type injector. This will help to compute the nozzle performance numerically at a particular section. It can be observed from the figure that as the value of ALR increases, the positive skewness of size distribution continuously decreases i.e., decrease in the droplet size with ALR values. Similar observations are made for both types of injectors. The subfigures clearly show that the distribution of the overall size at a particular section perfectly follows the lognormal distribution. While the overall velocity distribution doesn't follow any particular distribution, which was expected to follow the normal distribution. This can be seen in Fig. 11.

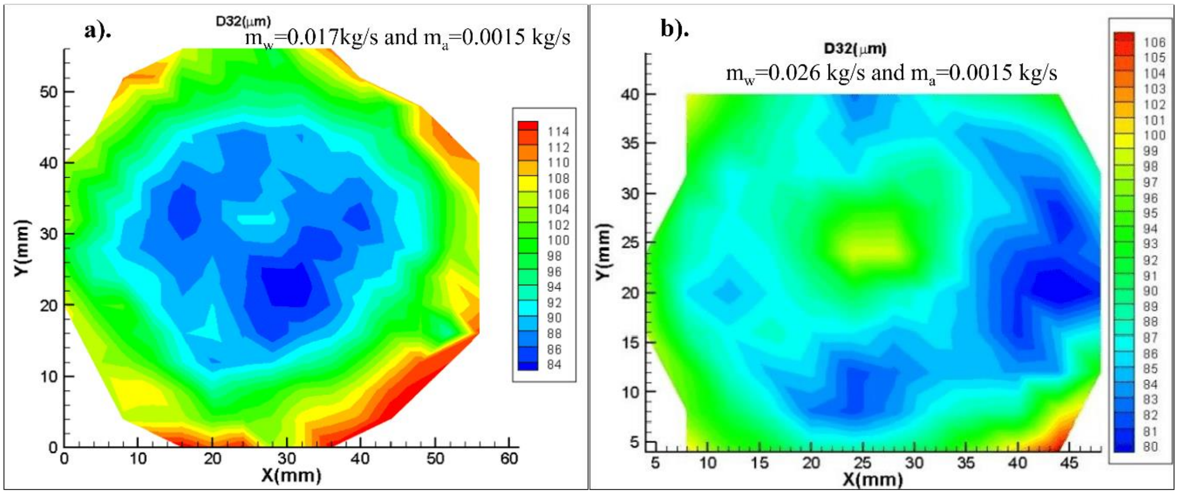

Fig. 5. SMD distribution at distribution at for a) 4 holes and b) 3 holes injector.

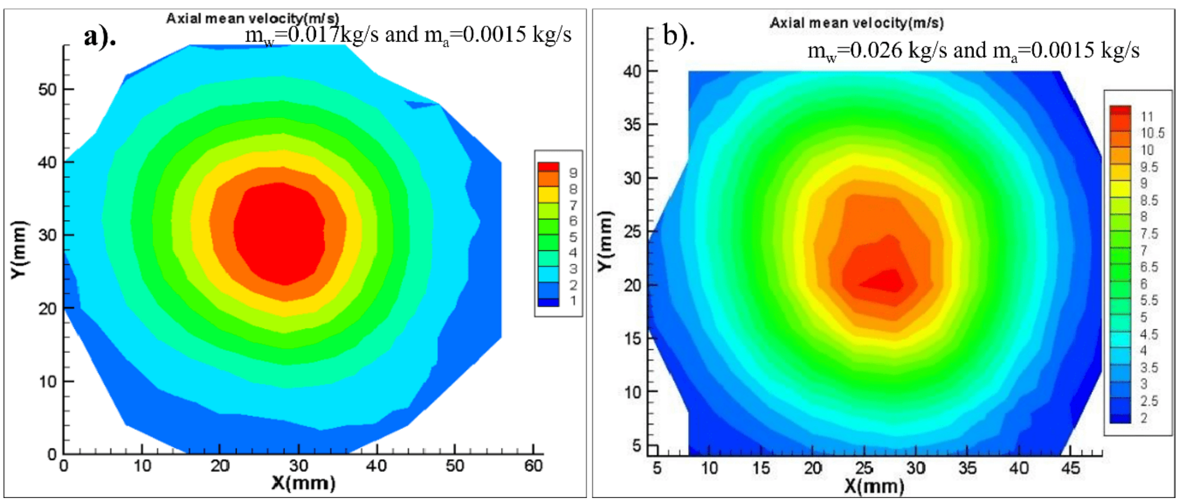

Fig. 6. Droplet axial mean velocity distribution at for a) 4 holes and b) 3 holes injector).

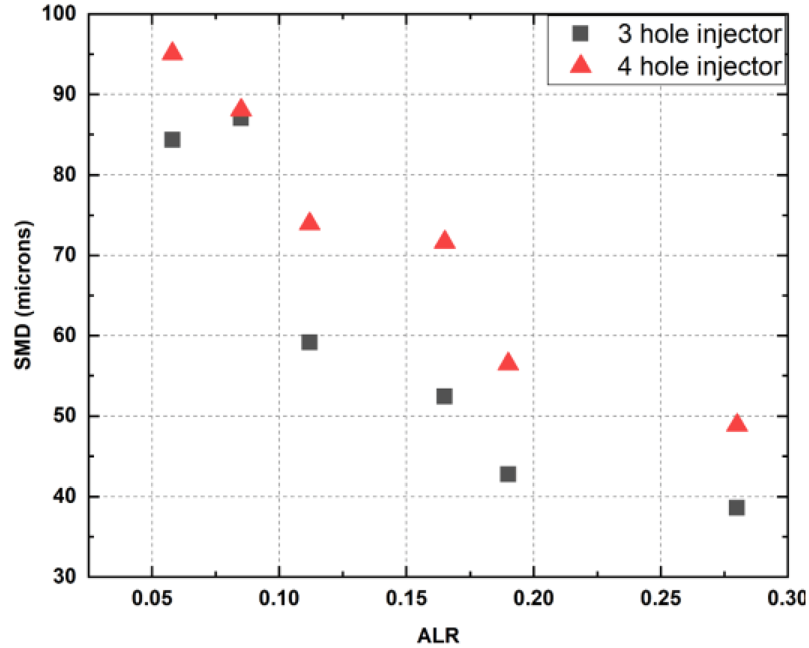

Fig. 7. Comparison of section-wise SMD between 3-hole and 4-hole injectors.

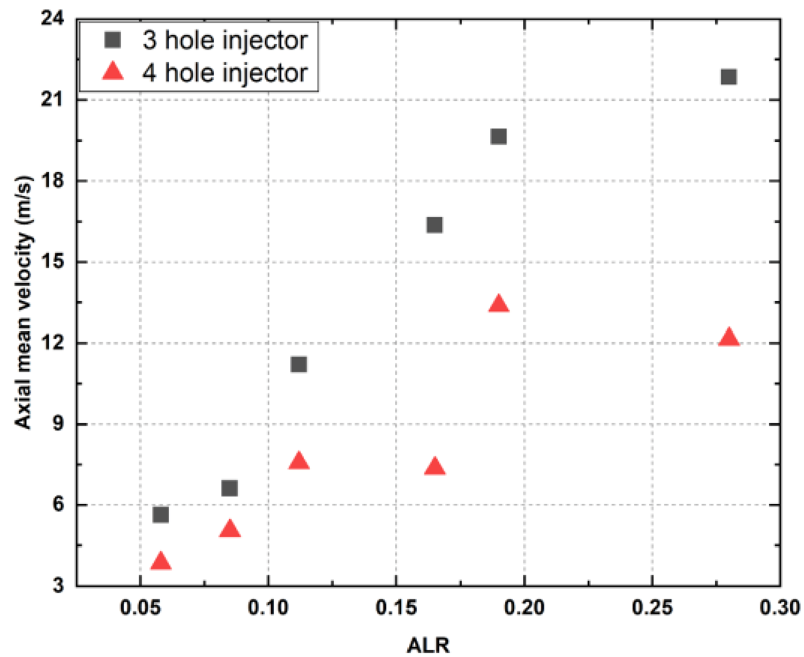

Fig. 8. Comparison of axial section wise mean velocity between the 3-hole hole and 4-hole injectors.

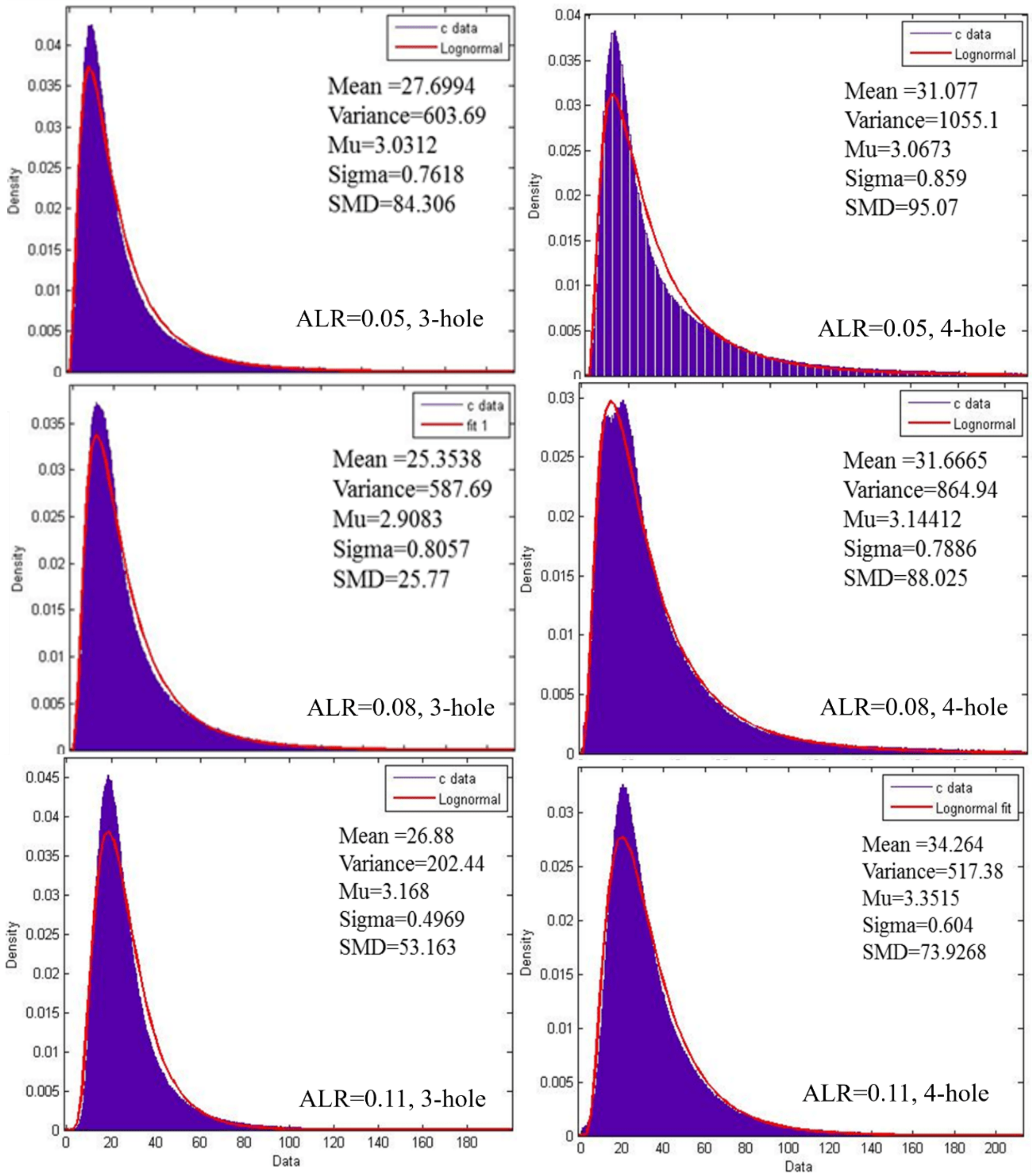

Fig. 9. Section-wise droplet size distribution for various ALR. First column- 3 hole and second column – 4-hole injector.

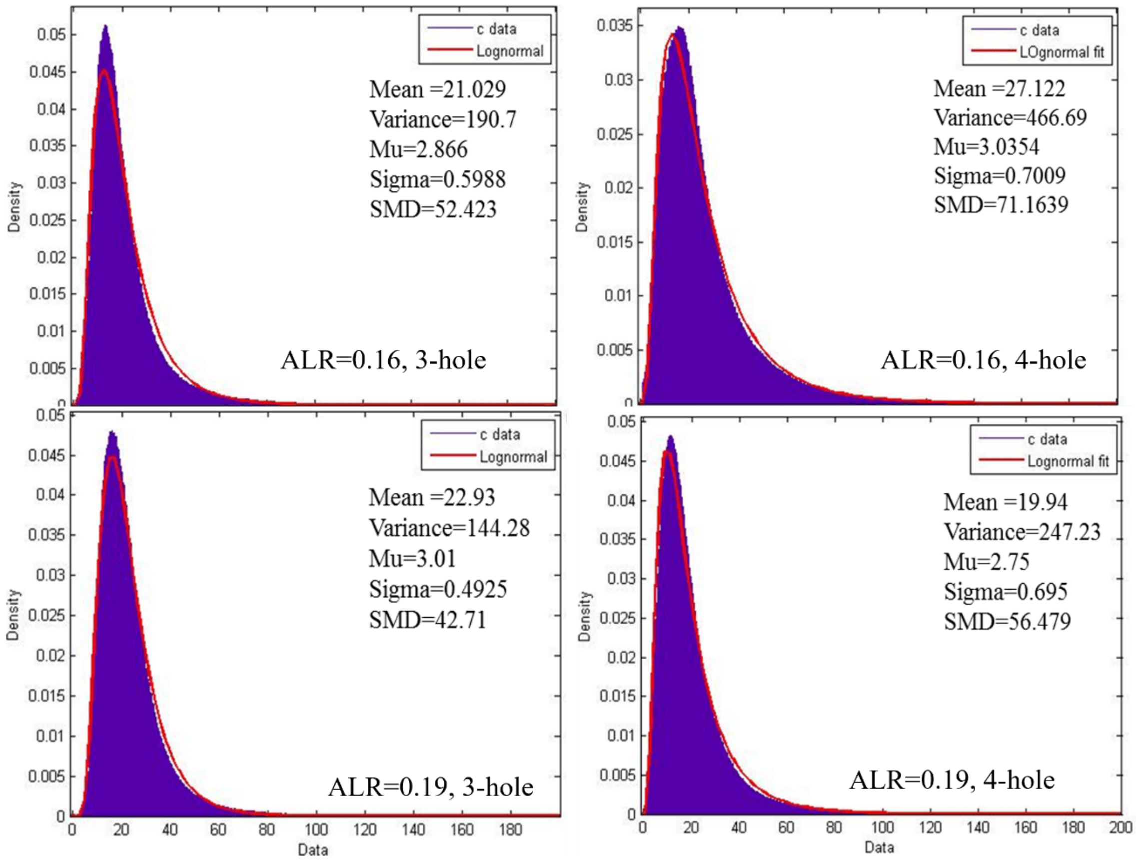

Fig. 100. Section-wise droplet size distribution for various ALR. First column- 3 hole and second column – 4-hole injector.

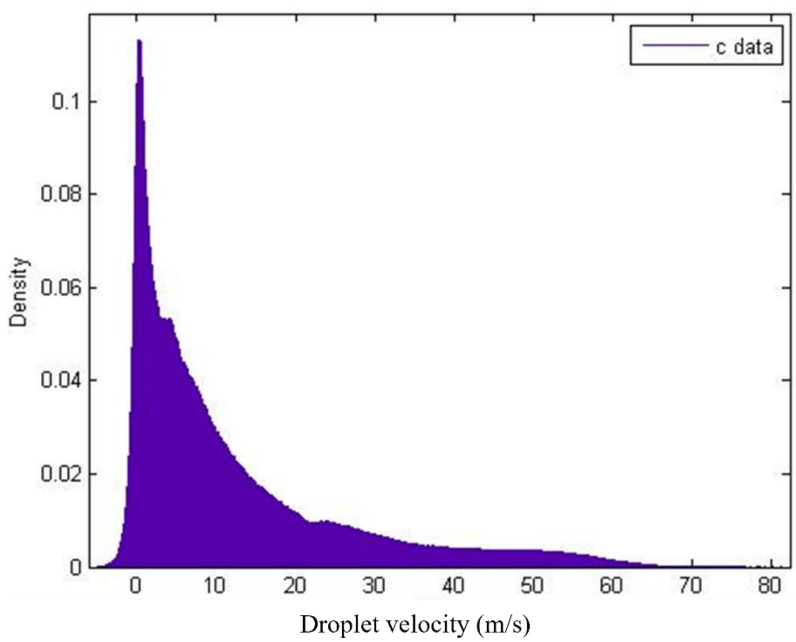

Fig. 111. Section-wise droplet axial velocity distribution.

4. Conclusion

A twin fluid injector was designed and developed for the modern FCC riser application by introducing the impactor plate. A comparative experimental study has been performed to evaluate the spray characteristics for 3-hole and 4-hole injector. For both three holes and four holes injector, it is observed that the spray velocities found maximum at the spray centerline and decrease as one moves along the radius of the spray. The 4-hole injector provides better atomization with smaller, more evenly distributed droplets, ensuring efficient mixing with the surrounding gas phase.

The 3-hole injector results in larger droplets that maintain higher velocities, leading to less uniformity and potential inefficiencies in combustion or catalytic cracking applications**.** The variation of SMD along the spray cross-section also shows a similar trend. This shows that smaller droplets have high axial velocities and fewer radial velocities which are negligible compared to the axial droplet velocities. Larger particles show high radial velocities and fewer axial velocities compared to the small droplets. For a fixed airflow rate, as the water mass flow rate is increased, there is very little variation in the droplet velocities. But for a fixed water mass flow rate as the air mass flow rate is increased, the droplet axial velocity and radial velocity are increasing (the kinetic energy of the air increases thus providing higher energies for the droplets). On the other hand, for a fixed mass flow rate of air as the water mass flow rate is increasing, the SMD is also increasing. But for a fixed mass flow rate of water as the air mass flow rate is increased, the droplet SMD also decreases. This can be expected as it is evident from the velocity measurements that the kinetic energy of the air is more dominant than the kinetic energy of water in the atomization process. It is also observed that for the same ALR as the area is reduced (three holes nozzle) the droplet velocities are increasing and the droplet SMD is decreasing compared to a larger exit area (four holes nozzle). The section SMD for both the injectors decreases and section mean velocity increases with an increase in ALR value. It also concluded that the section-wise size distribution perfectly follows lognormal distribution while section-wise velocity doesn't follow any particular distribution.

Acknowledgements

None.

Nomenclature

ALR air to liquid mass ratio
Q force
$\dot{m}_a$ mass flow rate of air (kg/s)
$\dot{m}_l$ mass flow rate of liquid (kg/s)
ρ_a density of air
ρ_l density of liquid
D_{10} Arithmetic mean diameter
D_{32} Sauter mean diameter
W_e Weber number
R_e Reynolds number
P_a Air pressure (psi)
P_l Liquid injection pressure (Psi)

Subscripts
a gas
l liquid

Superscripts
\+ downstream of the spray
\- upstream of the spray

References

[1] A.H. Lefebvre, *Atomization and Sprays*. New York: Hemisphere Publishing Corporation of Taylor & Francis,1989.

[2] P.B. Venuto, E.T. Habib. Fluid Catalytic Cracking with Zeolite Catalysts. Marcel Dekker, New York. 1979.
[3] K.N. Theologos, A.I. Lygeros, N.C. Markatos. Feedstock atomization effects on FCC riser reactors selectivity. Chem Engg Sci. 1999;54(22):5617–5625.
[4] Mirgain C, Briens C, Pozo MD. Modeling of Feed Vaporization in Fluid Catalytic Cracking. Ind Eng. Chem Res. 2000;39(11):4392–4399.
[5] Gupta A, Rao DS. Model for the performance of a fluid catalytic cracking (FCC) riser reactor: effect of feed atomization. Chem Eng Sci. 2001;56(15): 4489–4503.
[6] Guo L.J., Li G.J., Chen, B., Chen, X.J., Papailiou, D.D., and Panidis, Th.; 2002, "Study on Gas-Liquid Two-Phase Spraying Characteristics of Nozzles for the Humidification of Smoke". Exp. Therm. Fluid Sci., 26: 715-722.
[7] Lefebvre A.H, Chin J.S., 1993 "Flow Patterns in Internal-Mixing, Twin-Fluid Atomizers". Atomization Sprays, 3(4):463–75.
[8] Kushari A, Neumeier Y, Israeli O, Lubarsky E, Zinn BT., 2001, "Internally Mixed Liquid Injector for Active Control of Atomization Process". J. Propul. Power, 4(17):878–82.
[9] Kushari A., 2010 "Effect of Injector Geometry on the Performance of an Internally Mixed Liquid Atomizer". Fuel Process Technol. 91(11):1650–4.
[10] Ju SC, Li XW., 1990, "Experimental study on Internal Mixing Sonic Flow Air Assist Atomizer for Heavy Oils". In: International Gas Turbine and Aeroengine Congress and Exposition, June 11, 1990–June 14, 1990. Brussels, Belg: ASME, p. T6.
[11] Kim S, Kondo S, Nishida K, Hiroyasu H.,1997, "Effects of Mixing Chamber geometry and flow on spray characteristics from an internal mixing twin-fluid atomizer. Int. J. Fluid Mech. Res, 24(1–3):76–87.
[12] Nguyen D.A., Rhodes M.J., 1998 "Producing Fine Drops of Water by Twin-Fluid Atomisation". Powder Technol. 99(3):285–92.
[13] Kufferath A, Wende B, Leuckel W., 1999 "Influence of liquid flow Conditions on Spray Characteristics of Internal-Mixing Twin-Fluid Atomizers". Int. J. Heat Fluid Flow, 20(5):513–9.
[14] Karnawat J, Kushari A., 2006, "Controlled Atomization Using a Twin-Fluid Swirl Atomizer". Exp. Fluids, 41(4):649–63.
[15] Karnawat J, Kushari A, 2008. "Spray Evolution in a Twin-Fluid Swirl Atomizer". Atomization Sprays 18(5):449–70.
[16] Ferreira G, Barreras F, Lozano A, Garcia JA, Lincheta E., 2009, "Effect of the Inner Twin-Fluid Nozzle with an Internal Mixing Chamber". Atomization Sprays. 19(9):873–84.
[17] Ferreira G, Garciia J.A, Barreras F, Lozano A, Lincheta E.,2009, "Design Optimization of Twin-Fluid Atomizers with an Internal Mixing Chamber for Heavy Fuel Oils". Fuel Process Technol.90 (2):270–8.
[18] Lal S, Kushari A, Gupta M, Kapoor JC, Maji S.,2010 "Experimental Study of an Air-assisted Mist Generator". Exp Therm. Fluid Sci. 34(8):1029–35.
[19] Broniarz-Press L, Ochowiak M, Rozanski J, Woziwodzki S.,2009, "The Atomization of Water-Oil Emulsions". Exp Therm Fluid Sci. 33(6):955–62.
[20] Kumar D, Sikroria T, Kushari A, Kumar P, G. Sriganesh, "A twin-fluid injector for FCC feed injection". Int J Petrochem Sci Eng. 2019;4(3):109–115.